Cluster Computing (2019) 22:S8351–S8361
https://doi.org/10.1007/s10586-018-1803-1

Relative entropy-based Kalman filter for seamless indoor/outdoor multi-source fusion positioning with INS/TC-OFDM/GNSS

Enwen Hu[1] · Zhongliang Deng[1] · Qingqing Xu[2] · Lu Yin[1] · Wen Liu[1]

Received: 28 November 2017 / Revised: 9 January 2018 / Accepted: 9 January 2018 / Published online: 29 January 2018

Abstract
The current single data source positioning navigation systems cannot meet the high precision and high reliability required for indoor/outdoor positioning service. In this study, based on an inertial navigation system, time-and-code division-orthogonal frequency division multiplexing ranging technology and a global navigation satellite system, a relative entropy-based Kalman multi-source fusion positioning model is developed. First, multi-source numerical observation data are filtered, and the outliers are processed in data layers to improve data source reliability and to extract stable observation data. Next, the degree of the multi-source data coupling is quantified in an information layer to analyze the multi-source information coupling degree and to develop a coupling degree factor and a Kalman fusion positioning model for multi-source heterogeneous information. Tests show that this method significantly improves system positioning, navigation stability and positioning precision.

Keywords TC-OFDM · INS · GNSS · Relative entropy · Indoor/outdoor seamless

1 Introduction

With the rapid development of mobile communication technology, our society has gradually transformed into a digitized society. Location information, particularly indoor location information, has become essential information in modern society. Indoor/outdoor location-based service (LBS) has become an essential service requirement for daily work and living, which is particularly the case in large and complex indoor environments, such as museums, airports, supermarkets, hospitals and underground mining areas. In the current mobile Internet era, 70% of the mobile phone-based voice connections, purchases, payments and data connections and 80% of the Internet data access occur in indoor environments [1,2]. These mobile applications directly or indirectly leverage indoor/outdoor location information. Indoor/outdoor location information has thus become an essential part of location big data (LBD) and has applications in various sectors (Fig. 1).

- *Intelligent transportation ILBSs* ILBSs can provide millions of real-time location information data points to achieve destination and traffic guidance [3].
- *Smart health ILBSs* remote health care and smart hospitals require precise indoor location information to support management [4].
- *O2O ILBSs* it is important for shops to capture the consumption habits from customers to exploit product marketing [5].
- *Modern logistics ILBSs* ILBSs can contribute continuous position fingerprinting to manage goods seamlessly [6,7].
- *Firefight emergency ILBSs* saving lives in a fire with a smart device requires a device to establish a safe path and reduce direction-related errors and positioning inaccuracies [8,9].
- *Mine management and rescue ILBSs* the positions of all miners are important for daily management and emergency rescue [10].
- *Anti-terrorism support ILBSs* indoor target sensation and detection can determine the position of terrorists in a building to achieve an accurate attack [11].
- *Smart museum ILBSs* to arrive at the desired place in the museum is straightforward under the guide of ILBSs [12].

✉ Enwen Hu
owenhu@bupt.edu.cn

[1] Electronic Engineering, Beijing University of Posts and Telecommunications, Beijing, China

[2] The College of Forestry, Beijing Forestry University, Beijing, China

Fig. 1 Promising services and applications urgent for indoor/outdoor LBD (IOLBD)

In outdoor environments, global navigation satellite systems (GNSSs), such as the global positioning system (GPS) and the BeiDou navigation satellite system, provide users a meter-scale LBS, which provides accurate positioning in outdoor spaces and has broad applications in everyday life [13,14]. However, in indoor environments, where people spend 80% of their everyday life, the satellite navigation signal is blocked by buildings and is significantly attenuated. Additionally, severe indoor multi-path effects cause the precision of the GNSS positioning to decline sharply or to fail to provide positioning and thus cannot meet the requirement of the indoor LBS [15,16].

In recent years, indoor high-precision positioning technology in buildings has gradually become a priority research topic. An increasing number of researchers strive to solve "the final mile" positioning problem for this service. Various technologies and positioning methods have emerged that include optical-based positioning, infrared positioning, acoustic positioning, ultra-wideband positioning and geomagnetic positioning. A series of research findings were achieved, and specific application requirements have been satisfied in some fields. However, these methods usually require additional hardware setup and thus a higher cost, with limited system portability. Therefore, they cannot provide the same level of standard and stable indoor LBS as outdoor LBS (using a satellite positioning system) for users in various sectors, including public users.

Widely deployed wireless networks (Wi-Fi, Bluetooth, etc.) support indoor positioning without any hardware change. However, positioning capability is limited, and precision is normally within the range of 3–10 m [17]. In addition, signal source positioning with a single wireless network does not support seamless and coordinated indoor/outdoor positioning because it fails to meet user requirements in terms of robustness and reliability. It is difficult for a single-source positioning system to improve the system positioning capability with a positioning algorithm alone.

Therefore, research has focused on multi-source fusion positioning, based on information fusion technology. Using this technology, the homogenous or heterogeneous navigation data are integrated from various navigation sources via a fusion algorithm to obtain the optimal fused positioning result. Compared with conventional single-source navigation, multi-source fusion navigation fully leverages the advantages of each navigation source, thus providing optimal positioning and navigation service. In a navigation system, to improve navigation positioning precision, a Kalman filter is often employed to calculate the navigation system error state. The optimal estimation of the error state is then used to correct the system. The standard Kalman filtering algorithm is a linear, unbiased, minimum error variance-based optimal estimation algorithm [18,19]. The goal of its application is to deduce the system state from the measurements via the state equation and the measurement equation of the dynamic measuring system, accounting for measurement noise. However, the system state equation is time-variant, and the state transition matrix contains navigation information and inertial component measurements. These parameters, with their accompanying errors, can cause inaccuracies in filter models. In addition, precisely estimating or measuring the statistical patterns of system noise and observation noise individually is difficult. Therefore, the conventional Kalman filter often diverges, resulting in inferior stability and reliability.

To address this problem, adaptive filtering technology is popularly employed. During filtering, the information in the observation data, online estimation and modification of the model parameters, noise statistical characteristics and state gain matrix are continuously leveraged to improve filtering precision and obtain optimal estimates of the object state. Currently, there are numerous algorithms for adaptive Kalman filters [20–23]. For example, in the variance adaptive compensation method, the covariance matrix of the model error is generated adaptively from observed information during the Kalman filtering process, ensuring that the residual forecast and the corresponding statistics maintain excellent coherent filtering. Next, based on the open window approximation method, the residual series from the previous step are used to estimate the covariance matrix of the observation vector and the covariance matrix of the state error. In recent years, many researchers have proposed error-resistant estimation-based adaptive solutions for the observation weight matrix and the state weight matrix [24–26]. To accommodate smart navigation, error-resistant estimation and state covariance matrix expansion model-integrated adaptive filtering, referred to as error-resistant adaptive filtering, is proposed. In this method, the least square error-resistant solution for the current epoch is used to eval-

uate the forecast information precision. On this basis, the forecast information is utilized properly. The majority of existing adaptive filtering algorithms, however, estimate state variables via the covariance matrices of the online estimation system noise and the observation noise. The disadvantages of this method include a complex algorithm structure and inferior stability in a complex indoor environment; hence, it is difficult for these algorithms to accommodate next generation smart navigation systems.

The following issues in multi-source fusion positioning persist: (1) the reliability of the data from multiple signal sources must be improved, (2) high precision and high reliability is required of the multi-source heterogeneous information. In this study, based on the embedded GPS, BeiDou chipset, inertial component and time-and-code division-orthogonal frequency division multiplexing (TC-OFDM) ranging techniques, a relative entropy-based multi-source fusion positioning model is proposed. Initially, the multi-source observation numerical data is filtered and the outliers are processed at the data layer to improve the data source reliability and to extract stable observation data. In the information fusion layer, the multi-source observation numerical data are considered, and the information behind the data is quantified. The actual state process of the observation target is obtained via calculation and deduction from the data and the data attributes. The couple degree of the multi-source information are analyzed to create the relative entropy of the multi-source heterogeneous information for autonomous smart positioning.

In Sect. 2, the state equations of various systems and the multi-system fusion positioning model are introduced. In Sect. 3, data layer preprocessing is presented, where outlier data are removed, and a reliable data source is supplied to the information layer. The relative entropy-based Kalman fusion positioning model is then derived in detail. In Sect. 4, the simulation analysis and test verification of the method are described. In Sect. 5, the conclusions of this study are discussed.

2 System model

2.1 Inertial navigation system (INS) and state equation

The INS is a dead reckoning navigation method that consists primarily of an accelerometer, a gyroscope and motion sensor module(s). The external system provides the initial position and velocity for the INS. The INS then processes and integrates the motion sensor information to update the current position and velocity continuously. The advantage of an INS is the following. When the initial condition is set, the current position, the direction and the velocity are determined without an external reference. By measuring the system acceleration and the angular velocity, the INS detects changes in position, velocity and posture. The error state equation for the psi-angle is as follows [27]:

$$\delta \dot{r}^n = \delta v^n - \omega_{en}^n \times \delta r^n, \tag{1}$$

$$\delta \dot{v}^n = -\left(\omega_{ie}^n + \omega_{in}^n\right) \times \delta v^n + \varphi \times f^n + \nabla^n + \delta g^n, \tag{2}$$

$$\dot{\phi} = -\omega_{in}^n \times \phi + \varepsilon^n, \tag{3}$$

where δr^n, δv^n and ϕ represent the position error, the velocity error and the posture error, respectively, ω_{in}^n is the n-frame angular velocity relative to the i-frame, ∇^n is the acceleration error, δg^n is the gravitational acceleration calculation error, and ε^n is the gyroscope random drift error. The error state of the INS state is as follows:

$$X_I = \left[\delta r^n,\ \delta v^n,\ \delta\varphi,\ \delta\alpha,\ \delta\varepsilon\right]^T, \tag{4}$$

where δr^n is the position error, δv^n is the velocity error, $\delta\varphi$ is the posture error, $\delta\alpha$ is the acceleration error, and $\delta\varepsilon$ is the gyroscope random drift error. The INS discrete state equation is as follows:

$$\dot{X}_I = F_I X_I + G_I W_I, \tag{5}$$

where F_I is the state transition matrix, G_I is the dynamic noise matrix, and W_I is the system process white noise matrix. The formulae are as follows:

$$F_I = \begin{bmatrix} F_{rr} & F_{rv} & 0 & 0 & 0 \\ F_{vr} & F_{vv} & [(C_b^n \cdot f^b)\times] & 0 & C_b^n \\ F_{\varphi r} & F_{\varphi v} & -[\omega_{in}^n \times] & -C_b^n & 0 \\ 0 & 0 & 0 & -1/\tau_a & 0 \\ 0 & 0 & 0 & 0 & -1/\tau_g \end{bmatrix}, \tag{6}$$

$$G_I = \begin{bmatrix} 0 & 0 & 0\,0 \\ 0 & C_b^n & 0\,0 \\ -C_b^n & 0 & 0\,0 \\ 0 & 0 & 1\,0 \\ 0 & 0 & 0\,1 \end{bmatrix}, \tag{7}$$

$$W_I = \left[\, N_a\ N_g\ N_{ca}\ N_{cg} \,\right]^T \tag{8}$$

where the state transition matrix F_I sub-matrix F_{rr}, F_{rv}, F_{vr}, F_{vv}, $F_{\varphi r}$, and $F_{\varphi v}$ and the coefficients C_b^n and f^b are calculated via the INS error model [28]; and N_a, N_g, N_{ca}, N_{cg} are the random noise and the correlation noise of the acceleration and the gyroscope. The INS is an autonomous system that neither depends on any external information nor radiates energy toward the external environment. Therefore, it is stealthy, unaffected by external electromagnetic interference,

capable of full-time operation in the sky, on the surface of the earth and even under water, under all weather conditions around the globe, with superior short-term precision and stability. However, as navigation information is calculated via the integral, the positioning error increases over time, and the long-term precision is inferior. Before use, a lengthy initial calibration is required.

2.2 TC-OFDM and GNSS integrated positioning

A TC-OFDM positioning system [29] is a mobile broadcast network-based wide area positioning system. It is also an integrated aerial-terrestrial high-speed data transport network. A TC-OFDM terrestrial network consists of TC-OFDM cellular base stations, whose primary functions are to achieve ground coverage using a TC-OFDM signal, which contains both a high-speed communication signal and a navigation signal in the same frequency spectrum. The power of the navigation signal is much lower than that of the noise, which ensures that the navigation signal will not interfere with normal communication service. Because it is emitted by a cellular mobile base station or a broadcast tower, the navigation signal synchronization precision between base stations is on the order of 3 ns (Fig. 2).

In an outdoor environment, TC-OFDM and GNSS are integrated for positioning. The pseudo-ranging equation is as follows:

$$\rho_i = \sqrt{(x - x_i)^2 + (y - y_i)^2 + (z - z_i)^2} + \delta t_u, \tag{9}$$

where ρ_i is the satellite or the TC-OFDM base station, δt_u is the clock error between the satellite or the TC-OFDM and the user, and $[x_i,\ y_i,\ z_i)]$ is the position of the satellite or the TC-OFDM base station. Therefore, the TC-OFDM and GNSS-integrated positioning observation equation is as follows:

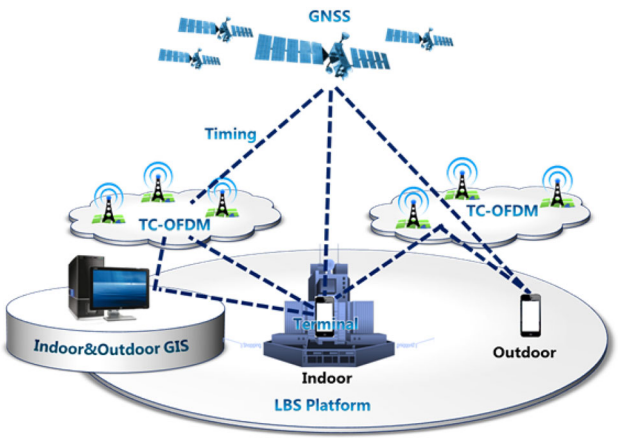

Fig. 2 The architecture of TC-OFDM system

$$V = AX_{T\&G} - L, \tag{10}$$

where

$$A = \begin{bmatrix} e_{11} & e_{11} & e_{11} & 1 \\ e_{21} & e_{22} & e_{23} & 1 \\ \vdots & \vdots & \vdots & \vdots \\ e_{31} & e_{32} & e_{33} & 1 \end{bmatrix}, \tag{11}$$

$$X_{T\&G} = \begin{bmatrix} \delta x & \delta y & \delta z & c \cdot \delta t_u \end{bmatrix}^T, \tag{12}$$

$$L = \begin{bmatrix} R_1' - c\delta t_u^1 - \rho_1 - l_1 \\ R_2' - c\delta t_u^2 - \rho_2 - l_2 \\ \vdots \\ R_n' - c\delta t_u^n - \rho_n - l_n \end{bmatrix}. \tag{13}$$

e_{1j}, e_{2j}, e_{3j} are cosines of the three directions from the satellite or the TC-OFDM base station to the receiver, R_i' is the ranging measurement, and l_i is the sum of the errors. Even though a satellite positioning system is very precise, economical and stable over the long term, when a carrier passes through a tunnel or is moving in a street surrounded by high-rise buildings, a signal blind zone cannot always be avoided with any combination of satellites. That is, there is no combination of navigation satellites that can completely eliminate all possible scenarios where the satellite signal is blocked. Therefore, continuous navigation in time and space is unattainable. On its own, the TC-OFDM supports indoor/outdoor seamless positioning navigation. It also covers the blind zones from the GNSS positioning in environments such as indoor, in urban canyons, under overpasses and in tunnels. Additionally, GNSS improves the outdoor positioning reliability of the TC-OFDM.

2.3 INS, the TC-OFDM and the GNSS loose coupling observation equation

This study is primarily based on an INS, TC-OFDM and GNSS loose coupling positioning mode. Therefore, a position–velocity combination-based INS/TC-OFDM/GNSS loose integration positioning model is created. The position, the velocity, the posture, the acceleration and the gyroscope drift error are the system state parameters. The formula is as follows:

$$X_k = \begin{bmatrix} \delta x,\ \delta y,\ \delta z,\ \delta v_x,\ \delta v_y,\ \delta v_z,\ \delta \varphi_x,\ \delta \varphi_y,\ \delta \varphi_z,\ \delta \\ \alpha_x,\ \delta \alpha_y,\ \delta \alpha_z,\ \delta \varepsilon_x,\ \delta \varepsilon_y,\ \delta \varepsilon_z \end{bmatrix}^T. \tag{14}$$

Based on formulae (X)–(X), the system continuous state equation is as follows:

$$\dot{X}_k = F_k X_k + G_k W_k \tag{15}$$

and the loose coupling observation equation is as follows:

$$Z_k = \Phi_k X_k + V_k, \tag{16}$$

where

$$Z_k = \left[\Delta x,\ \Delta y,\ \Delta z,\ \Delta v_x,\ \Delta v_y,\ \Delta v_z\right], \tag{17}$$

$$\Phi_k = \left[\, I_{6\times 6}\ 0_{6\times 9} \,\right], \tag{18}$$

$$\begin{cases} \Delta x = x_{ins} - x_{T\&G} \\ \Delta y = x_{ins} - x_{T\&G} \\ \Delta z = x_{ins} - x_{T\&G} \end{cases} \quad \begin{cases} \Delta v_x = v_{x,ins} - v_{x,T\&G}, \\ \Delta v_y = v_{y,ins} - v_{y,T\&G}, \\ \Delta v_z = v_{z,ins} - v_{z,T\&G}, \end{cases} \tag{19}$$

and $[\Delta x,\ \Delta y,\ \Delta z]$ and $[\Delta v_x,\ \Delta v_y,\ \Delta v_z]$ are the location difference and the velocity difference, respectively, between INS and TC-OFDM and GNSS, and V_k is the observation noise with variance R.

3 Relative entropy-based Kalman filter

In this paper, a relative entropy-based Kalman filter fusion positioning method is proposed. Outlier data are removed from the data layer to improve the observation data quality. For the fusion positioning model, a multi-source information coupling degree factor is proposed that changes the variable update equation in the conventional Kalman filter to improve the stability and fusion positioning precision of the filter. The architecture for this method is shown in Fig. 3.

3.1 Data layer preprocessing

There are outlier data in the raw positioning measurements that affect effective construction and positioning precision of the fusion model. Before the multi-source fusion positioning, the raw observation data is preprocessed to improve the data quality, efficiency, precision and performance of the fusion positioning process. In this paper, based on the short-term stability of the inertial output parameter, an inertial real-time observation-based data filtering method is proposed to obtain the system state equation extrapolation data as follows:

$$X_{k|(k-1)} = M X_{(k-1)} + Q \cdot X_I, \tag{20}$$

where

$$M = \left[\begin{matrix} I_6 & 0 \\ 0 & 0 \end{matrix}\right]_{15\times 15}. \tag{21}$$

The residual predicted by the system is as follows:

$$d_k = Z_k - \Phi_k X_{k|(k-1)}. \tag{22}$$

If d_k is the Gaussian random variable with an average of 0, the covariance matrix is as follows:

$$\in = E\left(d_k,\ d_k^T\right) = \Phi_k P_{k|k-1} \Phi_{k-1}^T + R_k, \tag{23}$$

where $P_{k|k-1}$ is the covariance matrix of forecast value $X_{k|(k-1)}$, and R_k is the observation noise. Therefore, the following formula determines if Z_i is an outlier:

$$d_{i,j} \in \left[-C\cdot \in_{j,j},\ C\cdot \in_{j,j}\right], \tag{24}$$

where $d_{i,j}$ represents the jth component of d_i, and C is the balance factor, which is typically 2 or 3.

3.2 Kalman filter based on relative entropy

Based on the data layer preprocessing, information fusion positioning must also consider the physical significance and attributes of the data. Therefore, a relative entropy-based coupling degree fusion model is proposed to create the relative entropy of the multi-source heterogeneous information and to update the Kalman filter posteriori estimation. The stability and the precision of the fusion model are significantly better

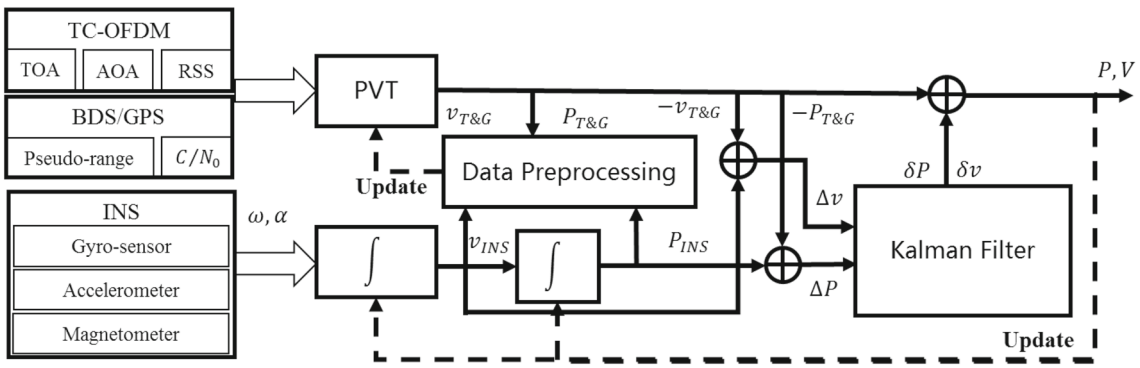

Fig. 3 Principle framework of relative entropy-based Kalman filter fusion positioning system

than those of the conventional Kalman filter. Based on the system continuous state equation developed in Sect. 2.3, the discrete Kalman state equation and the observation equation are as follows:

$$\dot{X}_k = F_{k|\mathrm{k}-1} X_{k-1} + G_{k-1} W_{k-1}, \tag{25}$$

$$Z_k = \Phi_k X_k + V_k. \tag{26}$$

In the forecast phase, the forecast value and the covariance matrix are as follows:

$$\hat{X}_{k|\mathrm{k}-1} = F_{k-1} \hat{X}_{k-1|k-1}, \tag{27}$$

$$P_{k|k-1} = F_{k-1} P_{k-1|k-1} F_{k-1}^T + Q_{k-1}. \tag{28}$$

If the state X_k follows a Gaussian distribution as follows:

$$f_x = N\left(x|\mu^-,\ P^-\right) \tag{29}$$

then the posterior is determined according to the following rule:

$$f_{x|z} \propto f_x N(z|\Phi,\ R). \tag{30}$$

For additive noise, the Kalman posteriori estimation is usually calculated via the general Gaussian filter (GGF) equation. In the update phase, the average and the variance of the posteriori value that follows a Gaussian distribution are estimated as follows:

$$\mu^+ = \mu^- + K\left(Z_k - Z_{k-1}\right), \tag{31}$$

$$P^+ = P^- - K \sum_Z \left(\left(Z_k - Z_{k-1}\right)\left(Z_k - Z_{k-1}\right)^T + R\right) K^T, \tag{32}$$

where $K$is the Kalman gain. In the GGF solution process, there is an implicit condition; i.e., the state variable X_k and the observation variable Z_k follow joint Gaussian distributions. The variables X_k and Z_k do not follow strict Gaussian distributions, however, which results in significant errors in the forecast or may even cause forecast divergence. Therefore, in this study, the estimation error is represented in relative entropy, and the coupling degree factor for $X_k$and Z_k is calculated as follows:

$$\aleph = KLD(X,\ Z) = \sum_X \sum_Z f_x \log f_x / f_{xz}. \tag{33}$$

The coupling degree factor represents the similarity between X_k and Z_k. A smaller coupling degree factor indicates a greater similarity between X_k and Z_k. Based on [30], $\aleph$ is as follows:

$$\aleph = \frac{1}{2} \log \left| I + R^{-1} \chi \right|, \tag{34}$$

where

$$\chi = \sum_X \sum_Z \left(\left(Z_k - Z_{k-1}\right)\left(Z_k - Z_{k-1}\right)^T - \Psi^T \left(P^-\right)^{-1} \Psi\right) \tag{35}$$

and

$$\Psi = \sum_X \sum_Z \left(X_k - \mu^-\right)\left(Z_k - Z_{k-1}\right)^T. \tag{36}$$

The coupling degree factor between the ith variable in the state vector X_k and the ith observation value inZ_k in a fusion positioning system is as follows:

$$\hat{\aleph}_i = \frac{1}{2} \log \left| I + R^{-1} \tilde{\chi}_{i,i} \right|, \tag{37}$$

where $\tilde{\chi}$ is the diagonal matrix of χ, defined as follows:

$$\tilde{\chi} = \varpi \chi \varpi^T. \tag{38}$$

The Kalman gain, the posteriori average and the variance are calculated from the coupling degree factor as follows:

$$\tilde{K} = \Psi \varpi^T \left(\sum_Z \left(Z_k - Z_{k-1}\right)\left(Z_k - Z_{k-1}\right)^T + R \right)^{-1}, \tag{39}$$

$$\tilde{\mu}^+ = \mu^- + \tilde{K}\left(Z_k - Z_{k-1}\right), \tag{40}$$

$$\tilde{P}^+ = P^- - \tilde{K} \sum_Z \left(\left(Z_k - Z_{k-1}\right)\left(Z_k - Z_{k-1}\right)^T + R\right) \tilde{K}^T. \tag{41}$$

To reduce computing resource consumption, a coupling degree factor threshold $\aleph_{threshold}$ is defined. All observation values smaller than $\aleph_{threshold}$ undergo Kalman iteration. The algorithm flow is shown in Fig. 4.

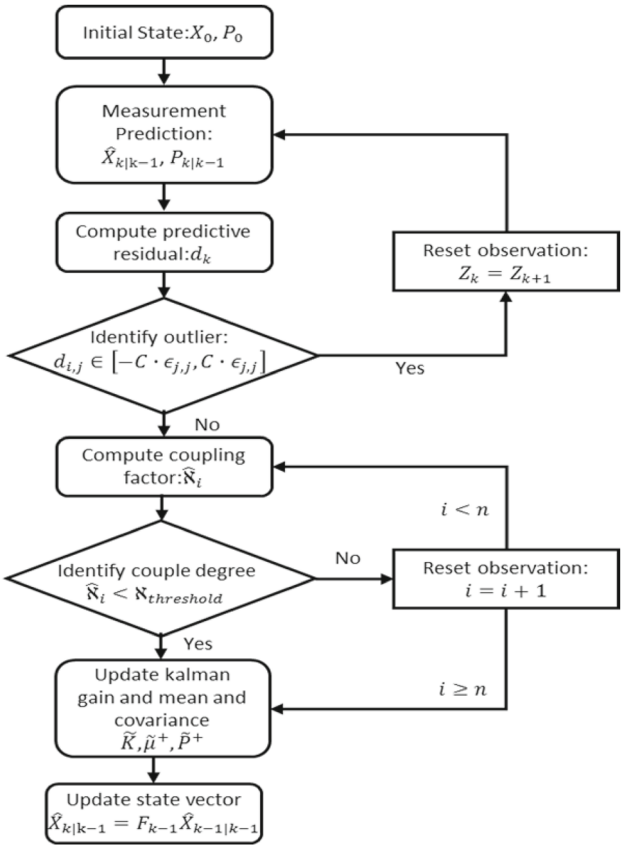

Fig. 4 Flow chart of the proposed method

3.3 Computation complexity analysis

The complexity of the computation of the fusion positioning algorithm is an important factor that affects the real-time positioning performance of integrated navigation systems. In this study, the complexity analysis considers floating point operations only. The computation complexity of the conventional Kalman filtering algorithm which comprises formula (27), (28) and (31)-(33) is as follows:

$$T(m) = 8n^3 + 10n^2m - n^2 + 6nm^2 - n + O\left(m^3\right). \quad (42)$$

The relative entropy-based Kalman filtering algorithm comprises formula (27), (28) and (36)–(43). Assume that the average fixed-point iteration number is T, and the complexity of the fusion positioning algorithm proposed in this paper is as follows:

$$\begin{aligned} T'(m) = {} & (8+4T)n^3 + (4+6T)n^2m - (2T-1)n^2 \\ & +(6+2T)nm^2 - (4T-2)nm + (6T-1)n \\ & +4Tm^3 + 2T\,O\left(n^3\right) + 4T\,O\left(m^3\right). \end{aligned} \quad (43)$$

Fig. 5 Test environment

4 Experiment

4.1 Experimental conditions

The indoor/outdoor positioning tests are performed at the Beijing University of Posts and Telecommunications, China. The indoor positioning test is performed in the National Science and Technology Innovation Park according to the plan shown in Fig. 5, where the base stations of TC-OFDM are marked. The positioning test uses the indoor/outdoor seamless positioning navigation device developed by our teams, which consists of a TC-OFDM module, an inertial component and a GNSS module, as shown in Fig. 5. The collected data initially undergo preprocessing and are compared with the actual data for analysis. To verify the effectiveness of the algorithm, data collected in the trials undergo simulation tests to compare the fusion positioning performance of various types of Kalman filters. Finally, the precision of the indoor and the indoor/outdoor seamless positioning navigation systems is tested (Fig. 6).

4.2 Data preprocessing of velocity and locations

The speed and locations are preprocessed in the outdoor environment of our campus for the integration of the positioning system, shown in the Figs. 8 and 9. In the speed data processing test, the green point in Fig. 7 is the velocity value obtained by the joint solution of TC-OFDM and GNSS. The orange line is the velocity value obtained by combining the inertial for preprocessing. From the Figs. 8 and 9, TC-OFDM and GNSS joint solution of the speed error is large, especially in the up direction. In addition, combined with the actual test route, we found that in the environments with occlusion, east and north direction speed error is larger. At this point with inertial auxiliary data processing is better.

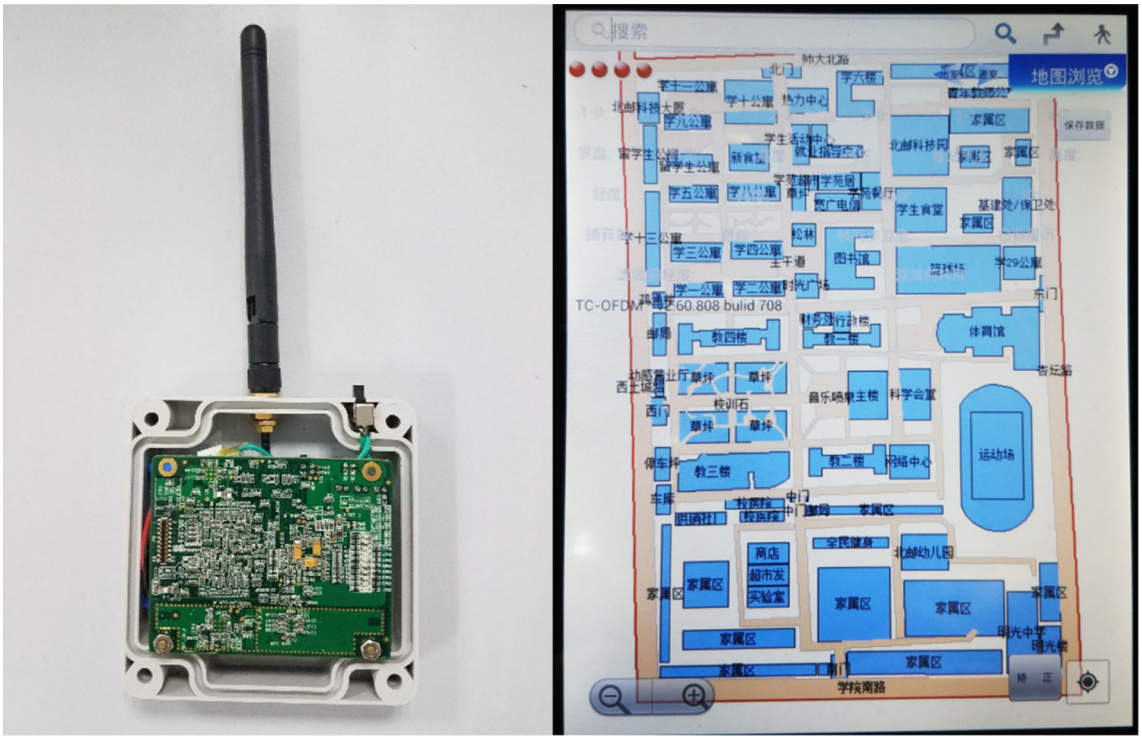

Fig. 6 Positioning receiver and indoor/outdoor positioning platform

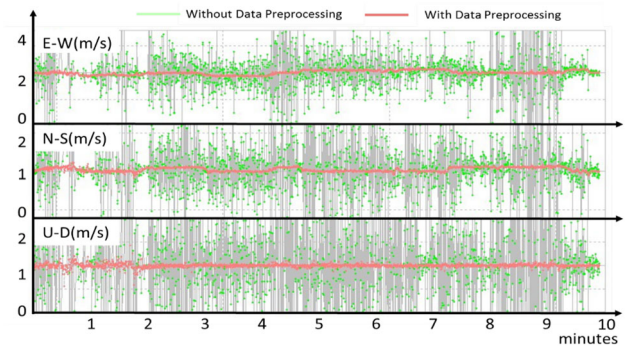

Fig. 7 Comparison of data filtering (position and velocity) (Color figure online)

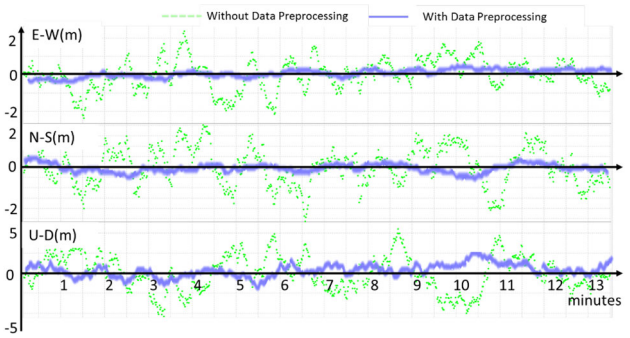

Fig. 8 Static point test

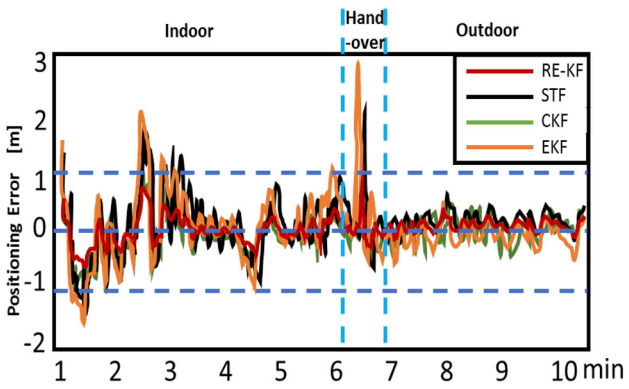

Fig. 9 Comparison of Kalman filter performance (Color figure online)

The static point test solution is applied to evaluate the performance of the data preprocessing method for location error. In a fixed point, continuous positioning for about 13 min is conducted. The green points are positioning results without preprocessing, as shown in Fig. 9. East and north direction error is of 1–3 m and up direction error of 1–5 m. The blue curve shows that the east and north direction errors is about 1 m and up direction error is of 1–3 m. Therefore, we can see that data preprocessing greatly enhance the positioning stability.

4.3 Performance of relative entropy based Kalman filter

The comparison of RE-Kalman, strong tracking filtering (STF) [31], cubature Kalman filter (CKF) [32], extended Kalman filter (EKF) [33] based fusion positioning model is shown in Figure 8. The first 6 minutes is tested in the indoor environments positioning accuracy, we can see from the figure 8 that the proposed method outperform better STF, CKF, and EKF, and with indoor positioning accuracy is better than 1 m, outdoor positioning accuracy of 0.5 m. In addition, in the process of indoor and outdoor switching, the positioning error of other fusion methods is larger than the method we proposed. Besides the RE-KF method we proposed is relatively more stable.

Figure 9 compares the GNSS/INS and TC-OFDM/GNSS/INS joint positioning to distinguish between green and orange lines. It can be seen from the figure that the former has a large error in tree-lined and high-rise, and even singular value, which is superior to the former in terms of accuracy and stability. Therefore, TC-OFDM system is combined with GNSS in outdoor environment, can make up for GNSS in the signal occlusion area deficiencies, greatly enhance the GNSS positioning performance.

5 Conclusion

In this paper, a relative entropy based indoor and outdoor seamless fusion method for TC-OFDM/GNSS/INS is proposed. Firstly, data preprocessing is carried out with the short stability of INS data to extract the more stable observations. Secondly, the coupling factor which based on the relative entropy between multi-source information is established, which the fusion performance of is greatly improved compared with traditional Kalman filter. Meanwhile, the complexity is consistent with the traditional Kalman filter method. The positioning is done by TC-OFDM/INS in the indoor environment and TC-OFDM/GNSS/INS fusion in outdoors, which enhances the positioning accuracy, stability and robustness of GNSS in the building around or the case of occlusion. The experimental data show that the method can realize the seamless positioning of indoor and outdoor, and the positioning accuracy is better than 1 m.

Acknowledgements The authors acknowledge the National Key Research and Development Program of China (Grant: 2016YFB0502001).

References

1. Cho, J., Yu, J., Oh, S., et al.: Wrong siren! A location spoofing attack on indoor positioning systems: the Starbucks case study. IEEE Commun. Mag. **55**(3), 132–137 (2017)
2. Hwang, I., Jang, Y.J.: Process mining to discover shoppers' pathways at a fashion retail store using a WiFi-base indoor positioning system. IEEE Trans. Autom. Sci. Eng. (2017). https://doi.org/10.1109/TASE.2017.2692961
3. Fernandez-Llorca, D., Minguez, R.Q., Alonso, I.P., et al.: Assistive intelligent transportation systems: the need for user localization and anonymous disability identification. IEEE Intell. Transp. Syst. Mag. **9**(2), 25–40 (2017)
4. Yin, Y., Zeng, Y., Chen, X., et al.: The internet of things in healthcare: an overview. J. Ind. Inf. Integr. **1**, 3–13 (2016)
5. Santoso, F., Redmond, S.J.: Indoor location-aware medical systems for smart homecare and telehealth monitoring: state-of-the-art. Physiol. Meas. **36**(10), R53 (2015)
6. Oosterlinck, D., Benoit, D.F., Baecke, P., et al.: Bluetooth tracking of humans in an indoor environment: an application to shopping mall visits. Appl. Geogr. **78**, 55–65 (2017)
7. Yang, Z., Zhang, P., Chen, L.: RFID-enabled indoor positioning method for a real-time manufacturing execution system using OS-ELM. Neurocomputing **174**(PA), 121–133 (2016)
8. Noh, Y., Yamaguchi, H., Lee, U.: Infrastructure-free collaborative indoor positioning scheme for time-critical team operations. IEEE Trans. Syst. Man Cybern. Syst. (2016). https://doi.org/10.1109/PerCom.2013.6526729
9. Zhang, X., Chen, Y., Yu, L., et al.: Three-dimensional modeling and indoor positioning for urban emergency response. Int. J. Geoinf. **6**(7), 214 (2017)
10. Luo, C., Fan, X., Ni, J., et al.: Positioning accuracy evaluation for the collaborative automation of mining fleet with the support of memory cutting technology. IEEE Access **4**, 5764–5775 (2017)
11. Friedman, J., Davitian, A., Torres, D., et al.: Angle-of-arrival-assisted relative interferometric localization using software defined radios. In: Proceedings of IEEE MILCOM, Boston, MA, USA, 2009, pp. 1–8
12. Alletto, S., Cucchiara, R., Fiore, G.D., et al.: An indoor location-aware system for an IoT-based smart museum. IEEE Internet Things J. **3**(2), 244–253 (2016)
13. Sun, C., Wu, Z., Bai, B.: A novel compact wideband patch antenna for GNSS application. IEEE Trans. Antennas Propag. (2017). https://doi.org/10.1109/TAP.2017.2761987
14. Yuan, X.M., Xin-Cheng, M.A., Sun, Y.Q.: The application of GNSS systems in bridge construction control. Geomat. Spat. Inf. Technol. **14**(5), 220–222 (2017)
15. Zhang, C., Li, X., Gao, S., et al.: Performance analysis of global navigation satellite system signal acquisition aided by different grade inertial navigation system under highly dynamic conditions. Sensors (2017). https://doi.org/10.3390/s17050980
16. Paul, A., Paul, K.S., Das, A.: Impact of multiconstellation satellite signal reception on performance of satellite-based navigation under adverse ionospheric conditions. Radio Sci. (2017). https://doi.org/10.1002/2016RS006076
17. Li, B., Khing, Y., Dempster, A.G.: Using two GPS satellites to improve WiFi positioning accuracy in urban canyons. (2013). https://www.researchgate.net/publication/267936200
18. Cheng, Y., Ye, H., Wang, Y., et al.: Unbiased minimum-variance state estimation for linear systems with unknown input. Automatica **45**(2), 485–491 (2009)
19. Chang, L., Hu, B., Chang, G., et al.: Huber-based novel robust unscented Kalman filter. IET Sci. Meas. Technol. **6**(6), 502–509 (2012)
20. Bian, H., Jin, Z., Tian, W.: Study on GPS attitude determination system aided INS using adaptive Kalman filter. Meas. Sci. Technol. **16**(16), 2072 (2005)
21. Lin, S.G.: Assisted adaptive extended Kalman filter for low-cost single-frequency GPS/SBAS kinematic positioning. GPS Solut. **19**(2), 215–223 (2015)

22. Tu, R., Wang, R., Walter, T.R., et al.: Adaptive recognition and correction of baseline shifts from collocated GPS and accelerometer using two phases Kalman filter. Adv. Space Res. **54**(9), 1924–1932 (2014)
23. Jwo, D.J., Wang, S.H.: Adaptive fuzzy strong tracking extended Kalman filtering for GPS navigation. IEEE Sens. J. **7**(5), 778–789 (2007)
24. Shi, Y., Sang, C., Gao, S.: Adaptive filtering for INS/SAR integrated navigation system. In: Asian–Pacific Conference on Synthetic Aperture Radar, 2009. APSAR 2009, pp. 884–887. IEEE (2010)
25. Zhu, W., Tang, J., Wan, S., et al.: Outlier-resistant adaptive filtering based on sparse Bayesian learning. Electron. Lett. **50**(9), 663–665 (2014)
26. Chen, B., Xing, L., Liang, J., et al.: Steady-state mean-square error analysis for adaptive filtering under the maximum correntropy criterion. IEEE Signal Process. Lett. **21**(7), 880–884 (2014)
27. Guo, H., Guo, J., Yu, M., et al.: A weighted combination filter with nonholonomic constrains for integrated navigation systems. Adv. Space Res. **55**(5), 1470–1476 (2015)
28. Ban, Y., Niu, X., Zhang, T., et al.: Modeling and quantitative analysis of GNSS/INS deep integration tracking loops in high dynamics. Micromachines **8**(9), 272 (2017)
29. Deng, Z., Yu, Y., Xie, Y., et al.: Situation and development tendency of indoor positioning. China Commun. **10**(3), 42–55 (2013)
30. Gultekin, S., Paisley, J.: Nonlinear Kalman filtering with divergence minimization. IEEE Trans. Signal Process. (2017). https://doi.org/10.1109/TSP.2017.2752729
31. Zhou, C., Xiao, J.: Improved strong track filter and its application to vehicle state estimation. Acta Autom. Sin. **38**(9), 1520 (2012)
32. Sun, F., Tang, L.J.: INS/GPS integrated navigation filter algorithm based on cubature Kalman filter. Control Decis. **7**, 1032–1036 (2012)
33. Liu, H., Meng, X., Chen, Z., et al.: A closed-loop EKF and multi-failure diagnosis approach for cooperative GNSS positioning. GPS Solut. **20**(4), 795–805 (2016)

Enwen Hu is currently working toward the PhD Degree in the Department of Electronic Science and Technology, Beijing University of Posts and Telecommunications, Beijing, China. His research interests include the compatibility and inter-operability of GNSS receiver, signal processing algorithms and FPGA implement.

Zhongliang Deng received the MSc Degree in Manufacturing Engineering from BeiHang University, and PhD Degree in Mechanical Manufacture from Tsinghua University, China. During 2002–2003, he was the Senior Visiting Scholar of Southern California University in USA. He is a Professor and Doctoral Supervisor at School of Electronic Engineering in Beijing University of Posts and Telecommunications now. He holds the position of Director of Research with the Laboratory of Intelligent Communication, Navigation and Micro/Nano-Systems (ICNMNS) since 2006. His research interests include indoor and outdoor seamless positioning, GNSS, satellite communications, MEMS and multimedia.

Qingqing Xu a Postgraduate, Majors in Remote Sensing Applications and Geographic Information System (GIS) in Beijing Forestry University. She has the great interest in our project of fusion positioning and deeply involved in data collection and analysis.

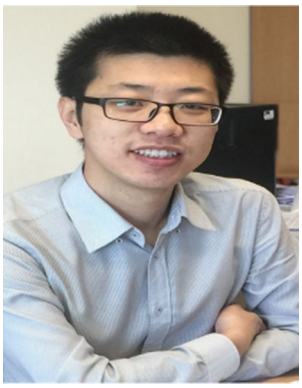

Lu Yin is currently working in the Department of Electronic Science and Technology, Beijing University of Posts and Telecommunications, Beijing, China. His research interests include GNSS, multi-system navigation receiver, combination navigation and indoor/outdoor seamless positioning.

Wen Liu received the PhD Degree from Beijing University, is currently working in the Department of Electronic Science and Technology, Beijing University of Posts and Telecommunications, Beijing, China. Her research interests include the position signal characteristics matching algorithms, MEMS and ASIC design.